Fish & Shellfish Immunology 33 (2012) 926–936

Contents lists available at SciVerse ScienceDirect

Fish & Shellfish Immunology

journal homepage: www.elsevier.com/locate/fsi

Ferritin H-like subunit from Manila clam (*Ruditapes philippinarum*): Molecular insights as a potent player in host antibacterial defense

Hyowon Kim [a,1], Don Anushka Sandaruwan Elvitigala [a,1], Youngdeuk Lee [a], Sukkyoung Lee [a], Ilson Whang [a,*], Jehee Lee [a,b,*]

[a] Department of Marine Life Sciences, School of Marine Biomedical Sciences, Jeju National University, Jeju Self-Governing Province 690-756, Republic of Korea
[b] Marine and Environmental Institute, Jeju National University, Jeju Special Self-Governing Province 690-814, Republic of Korea

ARTICLE INFO

Article history:
Received 24 May 2012
Received in revised form
13 July 2012
Accepted 1 August 2012
Available online 21 August 2012

Keywords:
Ferritin H
Manila clam
Recombinant protein
Iron chelating and antibacterial activity
Transcriptional profiling

ABSTRACT

Ferritins are iron chelating proteins, which involve in iron metabolism and sequestration, contributing to the iron homeostasis in living organisms. In the present study, one ferritin subunit which was identified as H-like subunit was completely characterized in cDNA and protein levels from Manila clam (*Ruditapes philippinarum*); (RpFeH). The full length cDNA of RpFeH was 776 bp and it consisted of open reading frame of 513 bp, encoding a 171 amino acid peptide with a calculated molecular mass of 19.6 kDa and isoelectric point of 5.23. The amino acid sequence resembled the characteristic features of typical ferritin H subunits, including seven metal ligands in ferroxidase center, two iron binding region signatures and potential bio-mineralization residue (Thy^{27}). Moreover, it was possible to identify an iron response element in 5′ untranslated region, showing an agreement with previously reported ferritin H like subunits. The generated 3 dimensional tertiary structure of RpFeH showed a substantial consistency with the human ferritin H subunit, reinforcing its validity. Recombinant RpFeH was overexpressed in *Escherichia coli* BL21 (DE3) and purified. The recombinant protein showed a detectable iron binding activity according to the results obtained in our iron chelating activity assay. Furthermore it showed a noticeable anti-bacterial activity through suppressing the growth of *Vibrio tapetis* bacteria. The quantitative real time PCR detected ubiquitous RpFeH expression in tissues examined. However expression was found to be elevated in hemocyte and gill tissues. Transcriptional profile of Manila clam gill tissue, challenged with *V. tapetis* demonstrated a prolonged significant ($P < 0.05$) transcriptional up-regulations from 12 h post injection to 48 h post injection. Our findings suggest that RpFeH functions as an iron chelating protein subunit in Manila clam while contributing to the innate immune responses against bacterial infections, via its iron withholding function.

1. Introduction

Micronutrients are essential, not only as intermediates in metabolism but also for crucial roles in living organisms such as wound healing, cellular immunity and antioxidant activity [1]. Among the essential micronutrients, iron plays a pivotal role in variety of cellular functions in biological systems including growth and differentiation, oxygen transport and storage, energy production, cell cycle and DNA synthesis, basically being a member of the active sites of many proteins and contributing to the electron transferring process in biochemical reactions [2–4]. However, iron can be considered as a double edged sword due to its deleterious effects, when it is present in excessive amount in the body, as well as due to its desirable effects. Iron is a catalyst for generation of reactive oxygen species (ROS) through different kinds of biochemical reactions, which are responsible for the oxidative damage in cellular environments [3,5]. Neurodegeneration is a grievous condition caused by the extremum of these reactions [6]. In order to prevent the cells from the above mentioned consequences, there should be a mechanism to sequestrate the excess iron in the body. In this regard, iron transport and storage proteins involve in a significant task, by maintaining the free form of the iron at safe concentrations [4].

Ferritin is an iron binding protein which is important in iron metabolism and sequestrating, in order to maintain the homeostasis

* Corresponding authors. Marine Molecular Genetics Lab, Department of Marine Life Sciences, College of Ocean Science, Jeju National University, 66 Jejudaehakno, Ara-Dong, Jeju Self-Governing Province 690-756, Republic of Korea. Tel.: +82 64 754 3472; fax: +82 64 756 3493.
E-mail addresses: ilsonwhang@hanmail.net (I. Whang), jehee@jejunu.ac.kr, jeheedaum@hanmail.net (J. Lee).
[1] These authors contributed equally to this work.

1050-4648/$ – see front matter © 2012 Elsevier Ltd. All rights reserved.
http://dx.doi.org/10.1016/j.fsi.2012.08.007

of the iron level in the body [4]. Ferritin is a hollow spherical protein complex of 24 subunits, comprising of a thick protein shell, which can mineralize up to 4500 iron atoms inside it [7]. Ferritin is mostly cytosolic but is also found in mammalian mitochondria and nuclei, in plant plastids and is secreted in insects [8]. In vertebrates the cytosolic ferritins are composed of Heavy (H) and Light (L) subunit types which have different molecular weights ranging between 18 and 28 kDa, encoded by two distinct genes [9,10]. The H subunit bears a catalytic iron binding site that makes up the ferroxidase center [11] whereas L subunit possesses amino acid residues known as the nucleation sites which provide ligands for binding Fe^{3+} ions [12]. Ferritin recognizes and binds two Fe^{2+} ions in the ferroxidase center where the Fe^{2+} ions are oxidized by di-oxygen to Fe^{3+} [13]. The assembly of H and L subunits in ferritins shows a tissue specific ratio that permits flexibility to adapt for cell needs [7]. Compared to the ferritin molecules enriched with L subunits, H-rich ferritins are more active in iron metabolism [11]. The H ferritin can translocate to the nuclei in some cell types to protect DNA from toxicity, or can be actively secreted, accomplishing various functions. The mitochondrial ferritin, found in mammals has a restricted tissue distribution and it seems to protect the mitochondria from iron toxicity and oxidative damage [7]. In lower vertebrates, a third subunit type designated as M subunit has been already reported, which possesses both the ferroxidase center of H subunit and iron nucleation sites of L subunit [7,14]. However recent reports demonstrate that ferritin is involved in several functions besides its role in iron metabolism and sequestration; such as cell activation, development, immunity and angiogenesis [15–18].

The expression of ferritin genes is regulated transcriptionally, as well as post transcriptionally, where the post transcriptional regulation is mediated by iron response proteins. The transcriptional profile of ferritin gene expression is found to be regulated by live pathogen or pathogen associated molecular pattern (PAMP) inductions [14], oxidative stress [14], inflammatory cytokines [19], iron loading [20], pH stress [21], temperature [22], and heavy metals [23]. Ferritins have been known to be involved in innate immunity in vertebrates and invertebrates through its characteristic iron withholding ability [24].

Ferritin can be found in variety of living organisms, including microorganisms, plants, vertebrates and invertebrates, sharing several conserved features [2,25]. Among invertebrates, mollusk ferritin subunits have been already identified and completely characterized in snail (*Lymnaea stagnalis*) [26], two oysters (*Crassostrea gigas* [27], *Pinctada fucata* [28]), two abalones (*Haliotis discus discus* [29], *Haliotis rufescens* [22]), bay scallop (*Argopecten irradians*) [30] and two clams (*Meretrix meretrix* [31] and *Sinonovacula constricta* [32]).

Manila clam (*Ruditapes philippinarum*) is a marine bivalve mollusk species, which resides in intertidal zones of East Asian countries such as Korea, Japan and China [33]. Greater demand of Manila clam as a delicacy throughout the world has contributed to the extensive growth of its economic value through the progression of their mariculture industry. However, the pathogenic threat on these bivalves due to various microorganisms, such as *Vibrio tapetis* has seriously affected to the yield of their mariculture production [34]. Therefore elucidation of the innate immune mechanisms in Manila clam has become a necessity, in order to launce appropriate operations to unriddle their pathogen menace.

The present study was performed with the basic objectives of structural and functional characterization of Manila clam ferritin H-like subunit (RpFeH) along with investigation of its transcriptional profile in tissue specific manner. In addition we determined its potential involvement in innate immune responses via transcriptional modulations upon time caused *V. tapetis* induction, along with monitoring the bacteriostatic activity.

2. Materials and methods

2.1. Identification of ferritin (H) subunit from clam cDNA database

The full length cDNA sequence, responsible for encoding ferritin H subunit in Manila clam was identified using the basic local alignment search tool (BLAST) (http://blast.ncbi.nlm.nih.gov/) from our previously established Manila clam cDNA sequence database [35] and designated as RpFeH (GenBank ID: JX286591).

2.2. Sequence characterization and phylogenetic analysis

The open reading frame and amino acid sequence of RpFeH were derived using DNAssist 2.2 (Version 3.0). The sequences of RpFeH from different species were compared by the BLAST search program. Pairwise sequence alignment and multiple sequence alignment were performed using the ClustalW2 program [36]. The phylogenetic relationship was determined using the Neighbor-Joining method under bootstrapping values taken from 1000 replicates and Molecular Evolutionary Genetics Analysis (MEGA) software version 5 [37]. Prediction of characteristic protein domains was carried out by the MotifScan scanning algorithm (http://myhits.isb-sib.ch/cgi-bin/motif_scan) and ExPASy-prosite database (http://prosite.expasy.org/). Some physicochemical properties of RpFeH were determined by expasy prot param tool (http://web.expasy.org/protparam).

2.3. Computer simulation modeling of RpFeH

The tertiary structure of RpFeH protein was modeled using I-TASSER online structure assembly simulation server [37] and the generated information of the model was represented as three dimensional (3D) structures using molecular structure visualizing software, Swiss-Pdb viewer version 4.0.4 [38].

2.4. Cloning of RpFeH open reading frame (ORF)

In order to clone and express the recombinant RpFeH (rRpFeH), pMAL protein fusion and purification system (New England Biolabs, USA) were selected. The coding sequence of the RpFeH was PCR amplified using corresponding cloning oligomers (Table 1), designed with the compatible restriction sites to the pMAL c2X vector (a maltose binding protein (MBP)-fused expression vector), *Eco*RI (N-terminus) and *Pst*I (C-terminus). The PCR was performed in a TaKaRa thermal cycler in a 50 μL total volume reaction mixture with 5 U of Ex Taq polymerase (TaKaRa, Japan), 5 μL of 10 × Ex Taq buffer, 8 μL of 2.5 mM dNTPs, 80 ng of template and 20 pmol of each

Table 1
Oligomers used in this study.

Name	Purpose	Sequence (5′ → 3′)
RpFeH-F	ORF amplification	gagagagaattcATGGCTGAATCAAGACCTCGCCA
RpFeH-R	ORF amplification	gagagactgcagCTAACCCTGAAGTTTCTGGTCGAAG
RpFeH-qF	Real-time PCR amplification for RpFeH	TCAAACATTCGGCAGACGAGGAGA
RpFeH-qR	Real-time PCR amplification for RpFeH	TTGTAACGCCGCTTTCATCGCATC
Rpβact-F	Real-time PCR amplification for β-actin	CTCCCTTGAGAAGAGCTACGA
Rpβact-R	Real-time PCR amplification for β-actin	GATACCAGCAGATTCCATACCC

primer. The reaction was carried out with an initial incubation at 94 °C for 3 min, followed by 35 cycles of 94 °C for 30 s, 57 °C for 30 s and 72 °C for 45 s, and a final extension at 72 °C for 5 min. The pMAL-c2X vector and amplified products were digested with corresponding restriction enzymes and analyzed on 1% agarose gel. Appropriate sized fragments were excised, purified using the Accuprep gel purification kit (Bioneer Co., Korea) and ligated into pMAL-c2X, by overnight incubation with Mighty Mix (TaKaRa) at 4 °C. The pMAL-c2X/RpFeH construct was transformed into *Escherichia coli* (*E. coli*) DH5α cells. The size of the construct and sequence of the coding region were confirmed by electrophoresis and sequencing, respectively.

2.5. Over expression and purification of recombinant RpFeH (rRpFeH) fusion protein

The recombinant fusion construct (rRpFeH-MBP) was transformed into *E. coli* BL21 (DE3) competent cells and a putative single transformant was grown overnight in a 250 mL LB broth, supplemented with 100 μg/mL ampicillin, at 37 °C with shaking (200 rpm). After the optical density at 600 nm reached to 0.6, isopropyl-β-thiogalactopyranoside (IPTG) was added at a final concentration of 1 mM and the mixture was incubated for 3 h at 25 °C to induce recombinant protein expression. Subsequently cells were cooled on ice for 30 min and harvested by centrifugation (3500 rpm for 30 min at 4 °C). The pellet was re-suspended in column buffer (20 mM Tris–HCl, pH 7.4 and 200 mM NaCl) and stored at −20 °C for overnight. After thawing, the cells were disrupted by cold sonication in the presence of lysozyme (1 mg/mL) and the resultant slurry was separated by centrifugation (9000 g for 30 min at 4 °C). The supernatant was defined as crude extract and the recombinant protein was purified using a pMAL protein fusion and purification technique [39]. After the purification, the concentration of the purified fusion protein product was determined using Bradford method [40] and purity was analyzed by 12% SDS-PAGE under reduced conditions.

2.6. Biochemical properties of RpFeH

In order to demonstrate the biochemical activity of RpFeH, its iron (II) chelating property was analyzed using the iron chelating assay, with the increasing concentrations of the recombinant fusion protein, according to a previously described protocol [41]. Briefly, purified rRpFeH fusion protein was dissolved in column buffer (20 mM Tris–HCl and 200 mM NaCl in 1 L) to increasing concentrations. Subsequently 20 mM $FeCl_2$ was added into 1 mL of protein suspension. After incubation at 22 °C for 10 min, 40 μL of 5 mM ferrozine was added to the solution. Following incubation at 22 °C for 15 min, optical density (OD) was measured at 562 nm.

2.7. Bacteriostatic activity analysis of RpFeH

In order to demonstrate the suppressive action of RpFeH on bacterial proliferation, purified recombinant RpFeH fusion protein with MBP was used against the growth of *V. tapetis* in marine broth medium, according to a previously published protocol, with some modifications [42]. Briefly, a *V. tapetis* culture, grown-up to reach 10^3 CFU/mL in marine broth, at 25 °C was used to add purified rRpFeH, until reaching its final concentration to 30 μg/mL in the solution. Subsequently culture was incubated at 25 °C and cell densities were measured by OD_{600} at different time points. To determine the effect of MBP in fusion protein on bacteriostatic action, MBP control was carried out. An additional assay was performed, adding the same volume of culture medium as a negative control to ensure the validity of the results. Every measurement was taken in three replicates in each assay.

2.8. Experimental animals and tissue collection

Healthy clams, averaging 35 ± 5 mm in size, were collected from the east coastal area of Jeju Island (Republic of Korea). Clams were maintained at 21 ± 1 °C in 80 L tanks with aerated sand-filtered seawater having salinity of 34 ± 1%. Animals were acclimatized to laboratory conditions for 1 week prior to experimentation. Clams were daily fed with commercially available marine microalgae mixture (Shellfish Diet 1800®, Reed Mariculture Inc) during both acclimation and experimental periods. Hemolymph (1–2 mL/clam) was collected from the posterior adductor muscle sinus of healthy, unchallenged clams using a 26 G syringe; samples were immediately centrifuged (3000 rpm at 4 °C for 10 min) to harvest the hemocytes. Tissues from adductor muscle, mantle, siphon, gill and foot were collected from three animals, snap frozen in liquid nitrogen and stored at −80 °C.

2.9. Immune challenge experiment

In order to determine the immune response of RpFeH for bacterial induction, a group of collected clams were challenged with *V. tapetis*, a Gram-negative bacterium. In this intact bacterial challenge, 100 μL of *V. tapetis* (1.9×10^9 cell/mL in saline) was injected into adductor muscle. A group of uninjected clams served as a negative control whereas another group injected an equal volume (100 μL) of saline was used as a positive control. Gill tissue was collected at 3, 6, 12 and 48 h post injection (p.i.) from control and challenged groups. Total RNA was extracted from tissues of at least five clams and used for cDNA synthesis.

2.10. Total RNA extraction and cDNA synthesis

Total RNA was isolated from tissues collected (Sections 2.8 and 2.9), using the Tri Reagent (Sigma–Aldrich, St. Louis, MO, USA). The mRNA was purified by using an mRNA isolation kit (FastTrack 2.0; Invitrogen, Carlsbad, CA, USA) following the manufacturer's instructions. Concentration was quantified by measuring the absorbance at 260 nm in a UV-spectrophotometer (Bio-Rad, Hercules, CA, USA). Purified RNA samples were diluted up to 1 μg/μL and pooled to perform multi-tissue cDNA synthesis. The Creator SMART cDNA library construction kit (Clontech Laboratories, Mountain View, CA, USA) was used to synthesize the first-strand cDNA from 1 μg of pooled mRNA, after which amplification was carried out with the Advantage 2 PCR kit (Clontech), according to the manufacturer's protocols, with an initial incubation at 94 °C for 3 min, followed by 30 cycles of 94 °C for 45 s, 60 °C for 45 s and 72 °C for 2 min, and a final extension at 72 °C for 7 min. The resultant double-stranded cDNA was diluted to 1:40 and stored at −20 °C until use for the quantitative RT-PCR.

2.11. RpFeH mRNA expression analysis by quantitative real time polymerase chain reaction (qRT-PCR)

qRT-PCR was used to analyze the expression levels of RpFeH. Total RNA was extracted at different time points following immune induction, and the first-strand cDNA synthesis was carried out as described in Section 2.10. qRT-PCR was carried out as described previously [43], using gene specific primer pair, RpFeH-qF and RpFeH-qR along with β-actin primers, Rpβact-F and Rpβact-R (Table 1). The expression level of siphon mRNA was considered as the basal level by which expressions in all other tissue were contrasted. To determine fold difference following challenges the

observed expression was compared with expression in the unchallenged group and normalized to the saline injected group. To determine statistical significance ($P < 0.05$) between the experimental and control groups, the two-tailed paired Student's *t*-test was carried out.

3. Results

3.1. Sequence characterization and phylogenetic analysis of RpFeH

The full length cDNA of RpFeH consists of 776 nucleotides (nt), which is comprised of 513 bp open reading frame (ORF) encoding 171 amino acids, 52 bp 5′ un-translated region (5′ UTR) and 209 bp 3′ un-translated region (3′ UTR). The 5′ UTR consists of an iron response element ($^{-50}$CCTTACTGGCTCAGTGAACGAAAGAAGG^{-23}) whereas 3′ UTR consists of a polyadenylation signal (^{619}AATAAA^{624}) (Fig. 1). Moreover the predicted molecular mass of RpFeH was around 19.6 kDa and theoretical isoelectric point was 5.23.

RpFeH comprised of seven amino acid residues designated as metal ligands in ferroxidase center, resembling the characteristic conserved feature in mammalian ferritin H subunit [25] (Fig. 1). Furthermore the deduced amino acid sequence of RpFeH contained two iron binding region signatures (IBRS) identified as ^{59}EEREHAEKLMKYQNKRGGRV^{78} and ^{124}DAQMSDFIEEEFLNEQVESIKE^{145} using PROSITE online server (http://expasy.org/prosite/). Potential bio-mineralization residue (Tyr^{27}) [44] could also be found in the derived amino acid sequence, manifesting the existence of novel RpFeH.

```
                A TCCTTACTG  CGTCAGTGA  ACGAAAGAA  GGAAGGACA  CAAAGTAAC  GATAAC     -52

ATGGCTGAA   TCAAGACCT   CGCCAAAAT   TTTCACCAG   GAGAGTGAA   GCTGGATTA   AACAAA      60
M--A--E--   S--R--P--   R--Q--N--   F--H--Q--   E--S--E--   A--G--L--   N--K--      20

CAGATTAAC   ATGGAATTA   TATGCCAGT   TATGTCTAT   CAATCAATG   GCCTACTAT   TTTGAC     120
Q--I--N--   M--E--L--   Y--A--S--   Y--V--Y --  Q--S--M--   A--Y--Y--   F--D--      40

AGAGATGAC   GTAGCGTTG   CCGGGATTC   TCGAAATTT   TTCAAACAT   TCGGCAGAC   GAGGAG     180
R--D--D--   V--A--L--   P--G--F--   S--K-- F--  F--K--H--   S--A--D--   E--E--      60

AGGGAACAT   GCAGAAAAG   CTGATGAAG   TATCAGAAT   AAACGAGGT   GGCCGTGTT   GTCCTA     240
R--E--H--   A--E--K--   L--M--K--   Y--Q--N--   K--R--G--   G--R--V--   V--L--      80

CAAGCTATA   CAAAAGCCG   GACCGTGAC   GAGTGGGGA   TCAGGCCTT   GATGCGATG   AAAGCG     300
Q--A--I--   Q--K--P--   D--R--D--   E--W--G--   S--G--L--   D--A--M--   K--A--     100

GCGTTACAA   CTAGAAAAG   ACCGTGAAC   CAGGCGCTT   ATCGACCTT   CACAATGTT   GCCAGT     360
A--L--Q--   L--E--K--   T--V--N--   Q--A--L--   I--D--L--   H--N--V--   A--S--     120

GGTCATGGC   GATGCACAG   ATGAGCGAT   TTCATCGAG   GAAGAATTT   CTGAACGAA   CAAGTC     420
G--H--G--   D--A--Q--   M--S--D--   F--I--E--   E--E--F--   L--N--E--   Q--V--     140

GAGTCGATT   AAGGAAATC   AGCGATCAC   GTGACCACA   TTGACTCGT   CTAGGAAGC   GGACAC     480
E--S--I--   K--E--I--   S--D--H--   V--T--T--   L--T--R--   L--G--S--   G--H--     160

GGAGAATGG   CACTTCGAC   CAGAAACTT   CAGGGTTAG   GAGTTGTTA   TGGACTGAT   GGGCTG     540
G--E--W--   H--F--D--   Q--K--L--   Q--G--                                     171

GTCTCATCA   AGTTTGATA   TATAGAATG   GCCGTTTCA   ACAGATACA   AATATGTGT   AATAAA     600

CGTCAACGT   TGCTTCAGT   TAATAAAAT   GTACCTGTG   TTCCTTGTA   ATACCCGGA   CTTTGT     660

CATAAAATA   TGTTTACTA   AGTAACCTA   TTTATTCTT   CGTTTTTAA   CTCCGATCT   ACAATT     720

CAAAA
```

Fig. 1. Nucleotides and deduced amino acid sequence of RpFeH. The start codon (ATG), the stop codon (TGA) and the polyadenylation signal sequence (AATAAA) are indicated by bold and underlining. The iron response element sequence was represented by bold letters in 5′ UTR. Gray shading depicts the seven metal ligands in the ferroxidase center. Putative ferritin iron binding region signatures (IBRS) 1 and 2 were denoted by double and single underlining, respectively. Tyr^{27} residue, important in bio-mineralization of iron was indicated using a box.

Pairwise and multiple alignments of amino acid sequence revealed that RpFeH is showing fairly high identities with invertebrate orthologues, for instance ferritin subunits of razor clam and tiger worm shared 77.2% and 69.8% identities, respectively (Table 2). Although RpFeH showed lower identities with vertebrate orthologues compared to invertebrates, those ferritin subunits were aligned with RpFeH, exhibiting considerable homology (Table 2 and Fig. 2). Phylogenetic analysis was carried out using Neighbor-Joining method comparing RpFeH with different vertebrate and invertebrate ferritin subunit members (Fig. 3). The tree revealed two main clusters as expected, invertebrate clade and vertebrate clade. RpFeH forms a clade with the small subgroup of other two clams, razor clam and hard clam, exhibiting a fairly high bootstrap value (65). Altogether, three of them positioned in the large sub-group of mollusks which is a sub clade of the main sub-group of invertebrates, affirming that RpFeH is originated from a common ancestor of invertebrates, further from mollusks (Fig. 3).

3.2. Modeled tertiary structure of RpFeH

The potential 3D model of the tertiary structure of RpFeH was generated using multiple threading alignment and assembly simulation approaches. Reliability of the structure prediction was confirmed by several parameters calculated by the software. The substantial percentage sequence identity values (54–61%) of the templates in the threading aligned region with the RpFeH sequence and the normalized Z-score values of the threading alignments exceeding 1 were the predominant evidences among them. Moreover, the algorithmic calculation of TM score showed 0.91 ± 0.06, further substantiating the higher accuracy of the model.

The predicted model resembled the characteristic features that could be identified in the revealed crystal structure of human ferritin H subunit using X-ray crystallography technique (1992356, 17070541). The anticipated 3D model of single monomeric H subunit molecule of Manila clam ferritin 3 consisted of five α helixes, designated as A, B, C, D and E from N terminal. The helix D contains a kink at position 137 (Fig. 4). The first four (A, B, C and D) helixes were arranged as a bundle which contains seven conserved amino acid residues to form ferroxidase center. Four of those residues (Glu-25, Glu-59, Glu-60, His63) were located at one metal binding site, out of two present inside the bundle, known as site A and the other 3 (Thr-32, Glu-105, Gln-139) were positioned at the remaining metal binding site, known as site B.

Table 2
Percent identity, similarity with gaps of RpFeH gene with ferritin subunits of other species.

Organism	Accession number	Identity (%)	Homology (%)	Gap (%)	Amino acids
Sinonovacula constricta (Razor clam)	ACZ65230	77.2	88.9	0.0	171
Crassostrea ariakensis (Suminoe oyster)	ACU25551	77.2	88.3	0.0	171
Meretrix meretrix (Asiatic hard clam)	AAZ20754	76.6	90.6	0.0	171
Crassostrea gigas (Pacific oyster)	AAP83793	76.6	88.3	0.0	171
Pinctada maxima (Gold lip oyster)	ACS72281	75.1	87.3	1.2	173
Mytilus edulis (Blue mussel)	AEM36072	71.3	83.0	4.1	164
Rhipicephalus microplus (Boophilus microplus)	AAQ54710	70.9	86.0	0.6	172
Dermacentor albipictus (Cattle tick)	AAQ54711	70.9	85.5	0	172
Haliotis diversicolor (Variously colored abalone)	ABY87353	70.8	86.5	0.0	171
Eisenia andrei (Tiger worm)	ACL14179	69.8	85.5	0.6	172
Haliotis rufescens (Red abalone)	ACZ73270	68.4	86.5	0.0	171
Ictalurus punctatus (Channel catfish)	AAY86949	60.1	76.4	4.5	177
Xenopus laevis (African clawed frog)	AAB20316	59.9	77.4	4.0	176
Salmo salar (Atlantic salmon)	AAB34575	59.6	77.0	4.5	177
Homo sapience (Human)	AAH66341	56.8	73.8	6.6	183
Gallus gallus (Chicken)	AAA48768	56.7	75.0	5.0	180
Bos taurus (Bovine)	NP776487	56.4	75.1	5.5	181

3.3. Purity of overexpressed rRpFeH

In order to analyze the purity of the rRpFeH, the overexpressed and purified rRpFeH fusion protein analyzed in a 12% SDS-PAGE in reduced conditions, along with the different fragments obtained in the intermediate steps of the purification procedure (Fig. 5). The SDS PAGE analysis indicated that the molecular mass of the purified rRbFeH was around 62 kDa, which was appeared as a single band. This observation was compatible with the molecular mass of predicted RpFeH (19.6 kDa), since the molecular mass of the MBP alone is around 42.5 kDa.

3.4. Iron chelating activity of rRpFeH

In order to demonstrate the iron binding activity of RpFeH, purified rRpFeH fusion protein was subjected to iron chelating assay which was designed based on color reduction of iron–ferrozine complex, along with purified recombinant MBP as the control. In accordance with data obtained, with the increasing rRpFeH concentration, OD_{562} values tend to be decreased, substantiating the protein concentration dependent formation of the iron–protein chelating complex, by binding more and more Fe^{2+} ions to the ferritin molecules rather than ferrozine (Fig. 6A). The highest binding activity was represented by the lowest OD value obtained at 562 nm (0.037), which was reported when the rRpFeH concentration was 7.2 μg/mL. In contrast to the control, MBP did not show any considerable drop of OD_{562} with its different concentrations used, indicating that MBP does not have any significant effect on the iron binding in the rRpFeH fusion protein.

3.5. Bacterial static activity of RpFeH

According to the graph obtained in bacterial static activity assay, rRpFeH showed a detectable inhibitive effect on *V. tapetis* growth, from 8 h post addition of the protein to the culture medium, reporting the OD_{600} value, around 0.8 in both controls. After 6 h, cell densities of bacteria were tended to elevate slowly in the protein introduced culture, compared to two controls, showing significantly lower ($P < 0.05$) OD_{600} values (0.76 and 0.80 at 8 h and 10 h respectively). However in early phase of the experiment the bacterial growth with the presence of the protein was overlapped with two controls, showing an elevated growth rate (Fig. 6B).

3.6. Tissue specific mRNA expression profile of RpFeH

In order to determine the tissue-specific transcriptional profile of RpFeH, qRT-PCR was carried out using gene specific primers and cDNA, synthesized by different tissues of Manila clam. The relative mRNA expression fold was calculated using the Manila clam β-actin gene (RpβAct) as a reference gene, further normalizing the expression of each tissue to the expression level of siphon. RpFeH mRNA was found to be constitutively expressed in all tissues analyzed, where significantly higher expression levels were

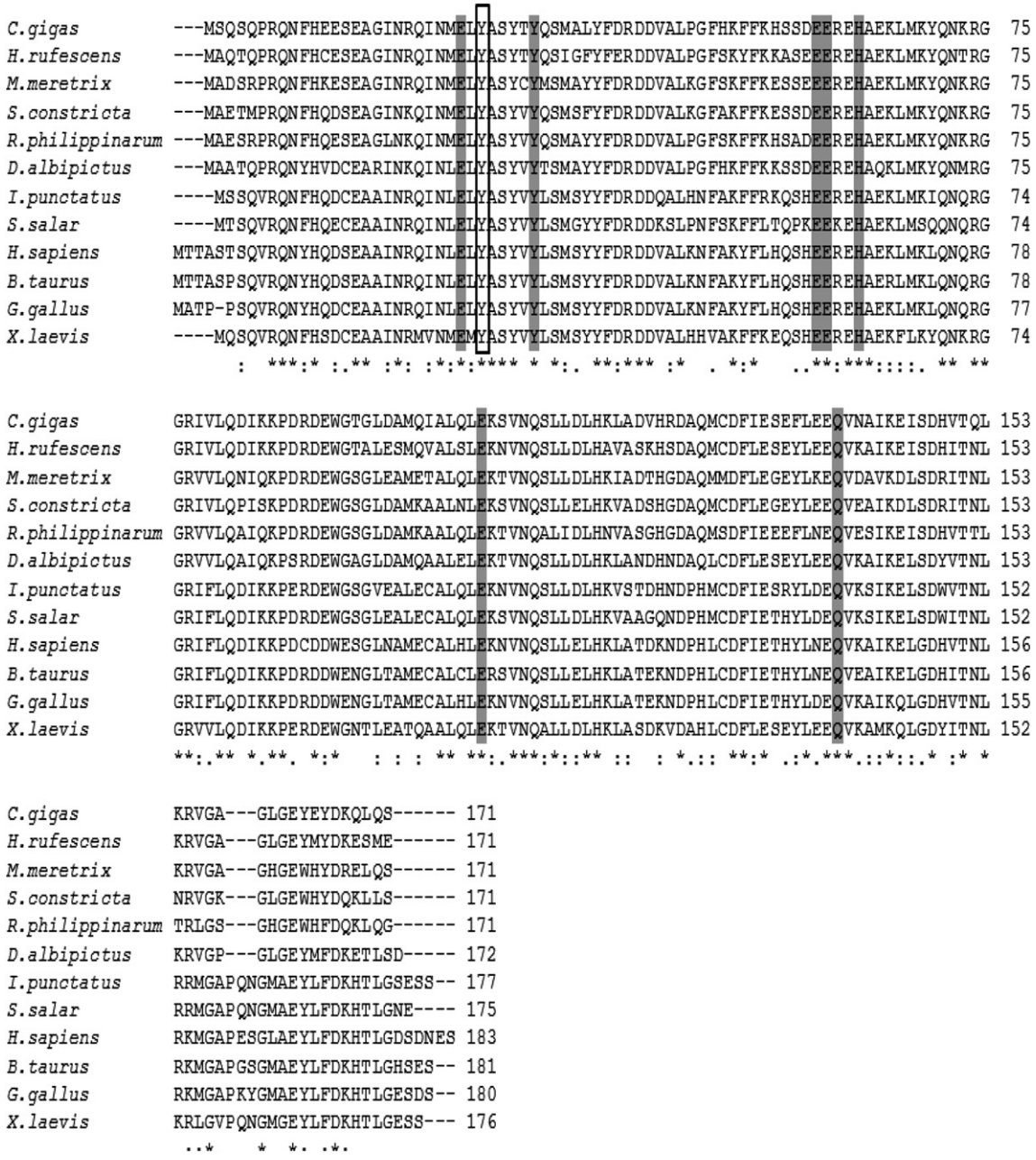

Fig. 2. Multiple sequence alignment of vertebrate and invertebrate ferritin H and H like subunits. Sequence alignments were obtained by the clustalW method. Conserved residues, important in metal binding and ferroxidation are shaded in gray color. Well conserved Tyr^{27} residue in bio-mineralization of iron is boxed. The complete scientific names of the animals, of which ferritin counterparts were used in the alignment, together with their respective accession numbers are given in Table 2.

observed in hemocyte and gill tissues. Moderately high RpFeH transcriptional profile could be identified in mantle and foot, whereas relatively low expression levels could be detected in siphon and mussel tissues of Manila clam (Fig. 7).

3.7. Transcriptional response upon bacterial challenge

In order to evaluate the transcriptional modulation of RpFeH upon *V. tapetis* induction, gill tissues from challenged clams were used. The relative mRNA expression fold changes were determined by normalizing the expression levels to the non-variant internal control RpβAct and further normalizing to the respective saline-injected controls at each time point. Expression level at 0 h time point was taken as the basal level.

According to the detected transcriptional profile upon the challenge, RpFeH transcript level was found to be significantly up-regulated ($P < 0.05$) at 12 h post injection (p.i.), marking its peak expression (~2.5 fold) level (Fig. 8). Similarly at subsequent time points (24 h p.i. and 48 h p.i.), the expression was detected to be significantly ($P < 0.05$) up-regulated (~1.4 and ~1.8 fold respectively), whilst those up regulations were subordinated compared to the expression level at 12 h p.i. (Fig. 8).

4. Discussion

Ferritin is a conserved and omnipresent iron binding protein, which mainly involves in iron metabolism and iron storing in bioavailable and nontoxic forms, contributing to sequestrate the

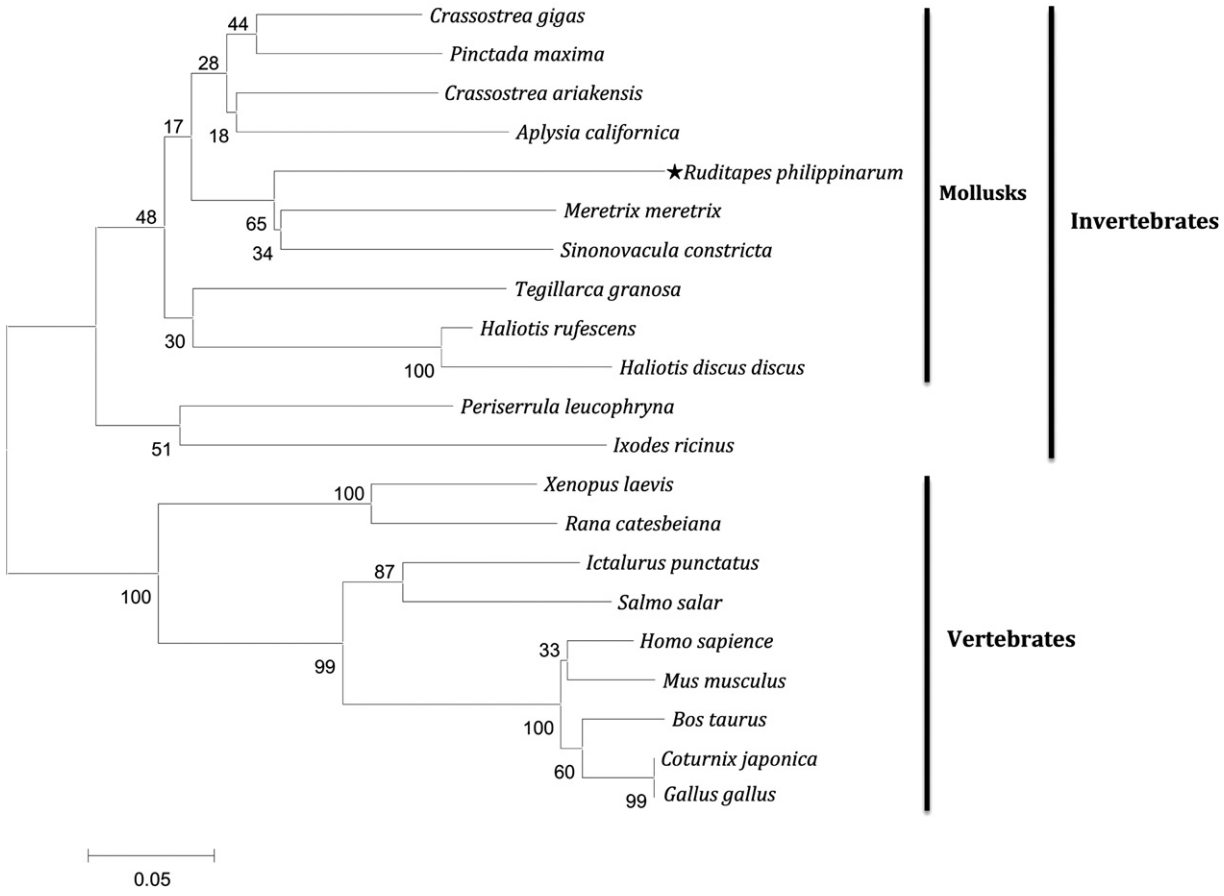

Fig. 3. Phylogenetic tree construct based on ClustalW alignment of deduced amino acid sequences of ferritin subunits of different animals, estimated by Neighbor-Joining method in MEGA version 5.0. Bootstrap values are shown on the lineages of the tree and major taxonomic clusters are indicated separately. The accession numbers are given in Table 2 with the exception *Aplysia californica* (ABF21074), *Ixodes ricinus* (AAN77903), *Tegillarca granosa* (ADC34696), *Periserrula leucophryna* (ABA55730), *Rana catesbeiana* (AAA49532), *Haliotis discus discus* (ABG88846), *Mus musculus* (NP034369) and *Coturnix japonica* (AAT01287).

excessive amounts of irons, in order to prevent cells from oxidative damage [45]. However, due to its iron withholding ability, ferritin can serve as a component in host innate immune defense, by restricting the bioavailability of iron for invading pathogenic microorganisms [46,47]. Hence, the characterization of ferritin protein-encoding genes and their regulation by pathogenic infections is important to launch better disease management strategies in aquaculture stocks. Nevertheless, studies on ferritin genes, especially relevant to its immune function from economically important marine invertebrates are relatively scarce. This article describes the ferritin H subunit in an important mariculture bivalve species, Manila clam, characterizing the corresponding gene in molecular level, while demonstrating its involvement and modulation in host defense.

According to the previous literature, ferritin subunits identified from most of the mollusk species consisted of amino acid sequences ranging 170–180 aa [30–32,48]. Interestingly, the coding sequence of RpFeH consisted of 513 nucleotides, encoding a peptide of 171 amino acids, identical to other two clam ferritins (*M. meretrix* and *S. constricta*) in amino acid number, affirming the agreement with its orthologous. Moreover RpFeH exhibited a highest identity (77.2%) with its counterpart of another clam *S. constricta*, convincing that the RpFeH is a novel member of the ferritin protein family (Table 1) in clams. Furthermore these counterparts have been claimed to be ferritin H subunits in previously published studies [31,32] due to the higher similarities with their ferritin H orthologues.

The multiple sequence alignment showed that the ferritin H subunit signatures are well conserved in RpFeH. Among them, seven amino acid residues form metal binding site and ferroxidase center showed significant conservation in vertebrate and invertebrate similitudes (Fig. 2). Besides these signatures, Thy^{27} which is a thoroughly conserved ferritin H specific residue, can also be identified in RpFeH protein [25]. Altogether, presence of these characteristic features, further absence of the iron nucleation site, corroborates that RpFeH is the 'H' Subunit of Manila clam ferritin, not L or M. In addition, according to the documented information, the characteristic highly conserved IRE motif was identified in RpFeH at the proximal site of the 5′ UTR (23 bp upstream from the start codon (ATG)), which is an important regulatory element as a binding site for the iron regulatory protein, for regulating the genes involve in iron metabolism [49]. The presence of this element provides evidence to the tight regulation of RpFeH expression.

Phylogenetic analysis of ferritin subunits from different vertebrate and invertebrate species generated a tree, in which a clear separation of two clusters as vertebrates and invertebrates could be identified. Mollusk ferritin subunit members clustered closely and independently, where RpFeH was placed with razor clam and hard clam, showing a bootstrap value of 65. However in vertebrate clade ferritin subunit (H) of bovine has been sub grouped with avian (chicken and Japanese quail) clade, deviating from mammalian clade (Human and mouse), convincing a relatively low sequence similarity with other considered mammalian counterparts, exhibiting an exceptional relationship.

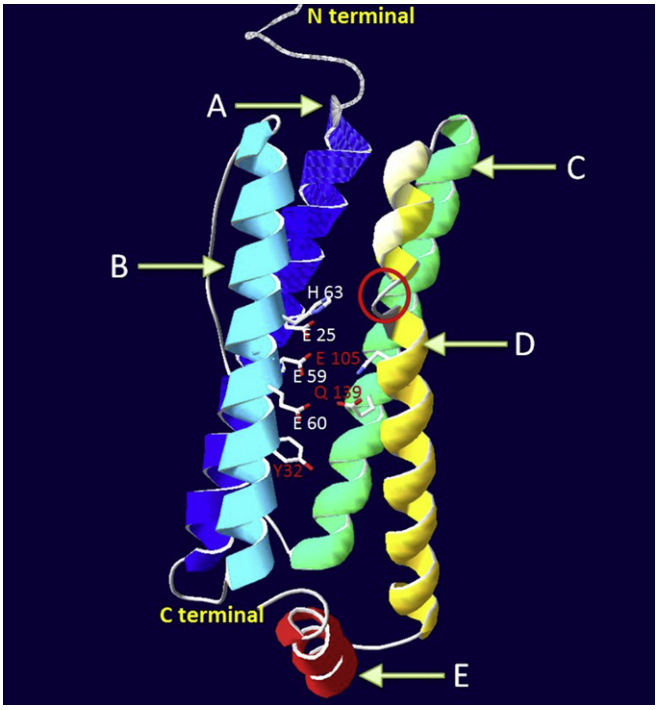

Fig. 4. Predicted 3D structural model of RpFeH. Five α helixes are labeled as A, B, C, D and E, starting from N terminal and the kink of helix D is indicated using a red color circle. The seven metal ligand residues important in metal binding and ferroxidation are represented by the side chains of each amino acid residue. White color labeled amino acids form metal binding site 'A' and red color labeled residues form the metal binding site 'B'. (For interpretation of the references to color in this figure legend, the reader is referred to the web version of this article.)

In our attempt in determination of the tertiary structure of the RpFeH revealed the typical ferritin H subunit structure depicting the features of metal binding and ferroxidase center, located in characteristic tetra helix bundle, substantiating the viability of RpFeH as a novel member of the ferritin family, further reinforcing the relationship between its structure and function.

Detected iron chelating activity of rRpFeH showed a concentration dependent elevation with the purified recombinant protein, supporting the structural prediction of its potential in iron binding. Our study provides the first evidence to the iron homeostasis function of a member of ferritin H family in clams.

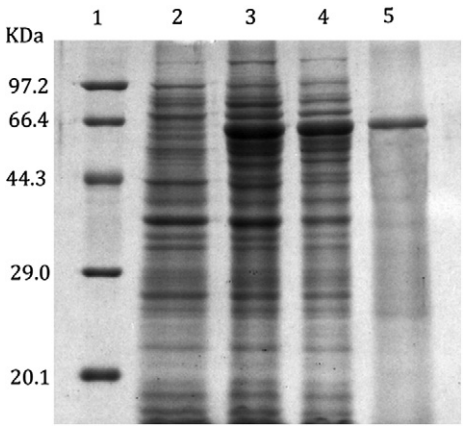

Fig. 5. SDS-PAGE analysis of overexpressed and purified recombinant RpFeH fusion protein. Lane 1, protein marker (TaKaRa); 2, total cellular extract from *E. coli* BL21 (DE3) prior to IPTG induction; 3, whole cell lysate; 4, crude extract of rRpFeH; 5, purified recombinant fusion protein (rRpFeH/MBP) after IPTG induction (1 mM) at 20 °C for 3 h.

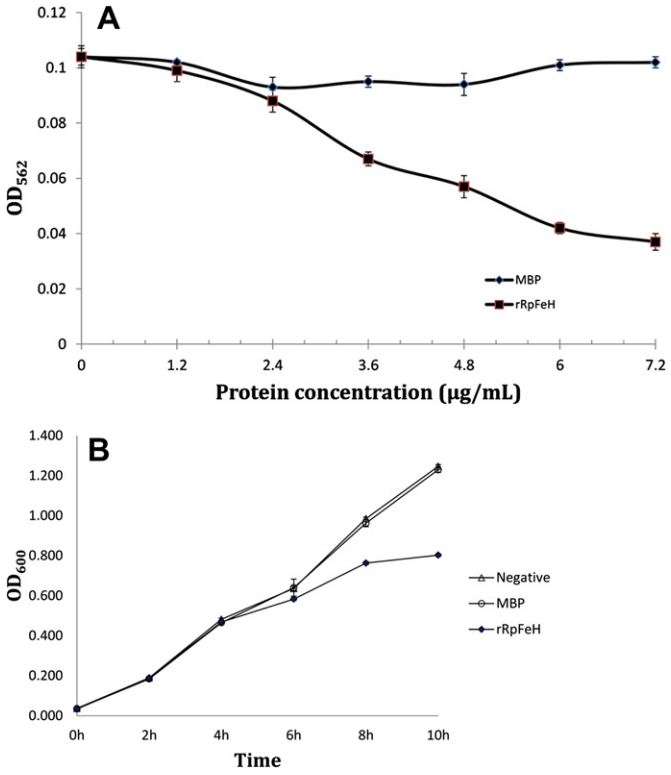

Fig. 6. (A) *In vitro* rRpFeH iron chelating assay. $FeCl_2$ was incubated with different concentrations of rRpFeH. Following the addition of ferrozine, OD_{562} was measured. (B) Effect of rRpFeH on the growth of *V. tapetis* bacteria. Bacterium was cultured in marine broth media with presence of rRpFeH (30 μg/mL), MBP (30 μg/mL) and absence of any protein, separately. Cell densities were monitored by measuring OD_{600} at different time points. Error bars represent the SD ($n = 3$).

RpFeH mRNA was found to be expressed ubiquitously in every tissue analyzed in our tissue distribution studies, albeit in different quantities, supporting the fact that ferritin is attributed to different roles in physiology, such as immune responses, shell formation and apoptosis, associate with iron levels in different tissue types [28,50,51]. Prominent expression levels of RpFeH were detected in gill and hemocyte among those tested clam tissues, where gill showed the highest expression (Fig. 8). This is an agreement with the previous studies on mollusk ferritin subunits from *Tegillarca granosa*, *H. discus discus* (Abf2), and *C. gigas* [27,29,52]. Furthermore, fairly abundant ferritin transcriptional level was also detected in visceral mass of Chinese razor clam, which contains most of the tissues of razor clam, including gill and hemocyte. The predominant transcript level in gills of above mentioned mollusks, including Manila clam, may be attributed to the role of ferritin in gaseous exchange process [53]. However in vertebrates, especially in fish and mammals, H ferritins were reported to be abundantly transcribed in liver and heart respectively, where iron metabolism is prevailingly taking place [3,54–56]. In accordance with the transcriptional response upon *V. tapetis* immune challenge, significant up-regulations could be detected in gill, at each time point, from 12 h p.i., corroborating that RpFeH is a candidate gene for Gram negative bacterial inductions. More or less compatible transcriptional modulation patterns were already experienced in different tissues in several marine invertebrate species upon gram negative bacterial challenges, such as hemocyte of bay scallop by *Listonella anguillarum* [30] and heart and hepatopancreas in horse shoe crab by *Pseudomonas aeruginosa* [46]. Moreover, in marine vertebrates, such as large yellow croaker [57], turbot [42], Atlantic cod [58] and

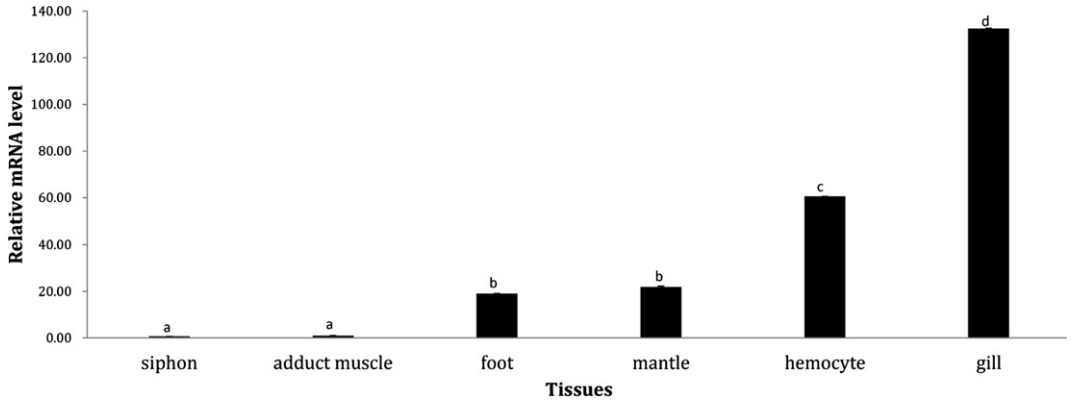

Fig. 7. Tissue expression analysis of RpFeH mRNA determined by quantitative real time PCR. Error bars represent the SD ($n = 5$). Data with different letters are significantly different ($P < 0.05$) among different tissues.

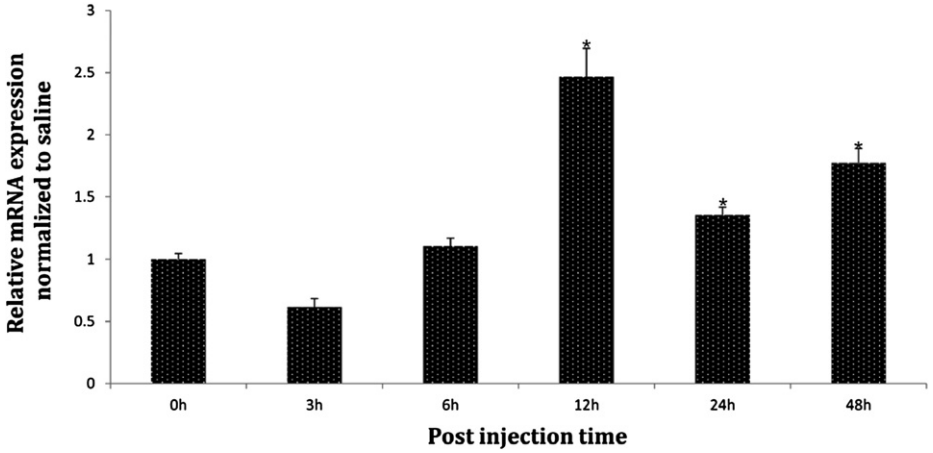

Fig. 8. Expression profile of RpFeH in gill tissue upon stimulation with *V. tapetis* bacteria. The relative expression was calculated by the $2^{-\Delta\Delta CT}$ method using Manila clam β-actin as reference gene with respect to corresponding saline controls at each time point. The relative expression fold at 0 h post-injection (p.i.) was kept as the basal line. Error bars represent the SD ($n = 5$); $^{*}P < 0.05$.

channel catfish [59], ferritin H transcript was augmented by stimulations of gram negative bacteria. Altogether, the above challenge responses, including our observation, gained credence through the underlying defense mechanism of iron withholding strategy in innate immunity [24]; further reinforcing the acute phase response of ferritins in bacterial infections.

Antibacterial activity of Manila clam ferritin H was further confirmed by our bacteriostatic activity assay, in which RpFeH exhibited a noticeable suppression of *V. tapetis* growth, 8 h after the introduction of the recombinant protein into the initial culture medium (Fig. 7). However compared to results observed in a previous report on the bacteriostatic activity of ferritin subunit in turbot [42], our protein has showed a late phase response, which may be attributed with the relatively lower concentration of rRpFeH used in our assay (30 μg/mL), whereas in turbot, 60 and 120 μg/mL of the recombinant purified protein concentrations were used separately in two assay trials. Overlapped graphs of OD_{600} value variation with the time in MBP introduced culture medium and the negative control divulged that MBP did not show any bacteriostatic activity in the fusion protein construct.

In summary, the complete cDNA sequence of ferritin H-like subunit from Manila clam was identified from our previously constructed cDNA library and structurally as well as functionally characterized along with analyzing its transcriptional profile in healthy and bacteria injected animals. Phylogenetic study disclosed the close evolutionary relationship of RpFeH with other invertebrate counterparts, further substantiating the prominent identity with clam similitudes. Recombinant purified RpFeH exhibited a detectable iron binding ability in our iron chelating activity assay resembling the characteristic biochemical property of typical ferritin H subunits. The response toward the *V. tapetis* bacterial challenge along with the antibacterial properties demonstrated by bacteriostatic assay found to be valuable evidences to the involvement of ferritin H in immune defense in Manila clam. Moreover the noticed iron cheating activity can be attributed to the immune related properties of RpFeH, based upon the iron sequestration strategy in innate immune mechanisms. However, in order to investigate the overall structure and function of Manila clam ferritin, it is necessary to carry out further analysis of other related subunits important in forming the complete protein, which will direct in identification of its dynamic roles in clam physiology and immunity.

Acknowledgment

This research was supported by Basic Science Research Program through the National Research Foundation of Korea (NRF) funded by the Ministry of Education, Science and Technology (2010-0014481).

References

[1] Visser J, Labadarios D, Blaauw R. Micronutrient supplementation for critically ill adults: a systematic review and meta-analysis. Nutrition 2011;27:745–58.
[2] Theil EC. Ferritin: structure, gene regulation, and cellular function in animals, plants, and microorganisms. Annual Review of Biochemistry 1987;56:289–315.
[3] Harrison PM, Arosio P. The ferritins: molecular properties, iron storage function and cellular regulation. Biochimica et Biophysica Acta 1996;1275:161–203.
[4] Watt RK. The many faces of the octahedral ferritin protein. Biometals: an International Journal on the Role of Metal Ions in Biology, Biochemistry, and Medicine 2011;24:489–500.
[5] McCord JM. Effects of positive iron status at a cellular level. Nutrition Reviews 1996;54:85–8.
[6] Friedman A, Arosio P, Finazzi D, Koziorowski D, Galazka-Friedman J. Ferritin as an important player in neurodegeneration. Parkinsonism & Related Disorders 2011;17:423–30.
[7] Arosio P, Ingrassia R, Cavadini P. Ferritins: a family of molecules for iron storage, antioxidation and more. Biochimica et Biophysica Acta 2009;1790:589–99.
[8] Crichton RR, Declercq JP. X-ray structures of ferritins and related proteins. Biochimica et Biophysica Acta 2010;1800:706–18.
[9] Orino K, Eguchi K, Nakayama T, Yamamoto S, Watanabe K. Sequencing of cDNA clones that encode bovine ferritin H and L chains. Comparative Biochemistry and Physiology Part B, Biochemistry & Molecular Biology 1997;118:667–73.
[10] Laulhere JP, Lescure AM, Briat JF. Purification and characterization of ferritins from maize, pea, and soya bean seeds. Distribution in various pea organs. The Journal of Biological Chemistry 1988;263:10289–94.
[11] Lawson DM, Artymiuk PJ, Yewdall SJ, Smith JM, Livingstone JC, Treffry A, et al. Solving the structure of human H ferritin by genetically engineering intermolecular crystal contacts. Nature 1991;349:541–4.
[12] Santambrogio P, Levi S, Cozzi A, Corsi B, Arosio P. Evidence that the specificity of iron incorporation into homopolymers of human ferritin L- and H-chains is conferred by the nucleation and ferroxidase centres. The Biochemical Journal 1996;314(Pt 1):139–44.
[13] Lawson DM, Treffry A, Artymiuk PJ, Harrison PM, Yewdall SJ, Luzzago A, et al. Identification of the ferroxidase centre in ferritin. FEBS Letters 1989;254:207–10.
[14] Zheng WJ, Hu YH, Sun L. Identification and analysis of a *Scophthalmus maximus* ferritin that is regulated at transcription level by oxidative stress and bacterial infection. Comparative Biochemistry and Physiology Part B, Biochemistry & Molecular Biology 2010;156:222–8.
[15] Wang W, Knovich MA, Coffman LG, Torti FM, Torti SV. Serum ferritin: past, present and future. Biochimica et Biophysica Acta 2010;1800:760–9.
[16] Alkhateeb AA, Connor JR. Nuclear ferritin: a new role for ferritin in cell biology. Biochimica et Biophysica Acta 2010;1800:793–7.
[17] Coffman LG, Brown JC, Johnson DA, Parthasarathy N, D'Agostino Jr RB, Lively MO, et al. Cleavage of high-molecular-weight kininogen by elastase and tryptase is inhibited by ferritin. American Journal of Physiology Lung Cellular and Molecular Physiology 2008;294:L505–15.
[18] Parthasarathy N, Torti SV, Torti FM. Ferritin binds to light chain of human H-kininogen and inhibits kallikrein-mediated bradykinin release. The Biochemical Journal 2002;365:279–86.
[19] Torti FM, Torti SV. Regulation of ferritin genes and protein. Blood 2002;99:3505–16.
[20] Wu C, Zhang W, Mai K, Xu W, Wang X, Ma H, et al. Transcriptional up-regulation of a novel ferritin homolog in abalone *Haliotis discus hannai* Ino by dietary iron. Comparative Biochemistry and Physiology Part C: Toxicology & Pharmacology 2010;152:424–32.
[21] Zhou J, Wang W, Ma G, Wang A, He W, Wang P, et al. Gene expression of ferritin in tissue of the Pacific white shrimp, *Litopenaeus vannamei* after exposure to pH stress. Aquaculture 2008;275:356–60.
[22] Salinas-Clarot K, Gutierrez AP, Nunez-Acuna G, Gallardo-Escarate C. Molecular characterization and gene expression of ferritin in red abalone (*Haliotis rufescens*). Fish & Shellfish Immunology 2011;30:430–3.
[23] Aziz N, Munro HN. Iron regulates ferritin mRNA translation through a segment of its 5′ untranslated region. Proceedings of the National Academy of Sciences of the United States of America 1987;84:8478–82.
[24] Ong ST, Ho JZ, Ho B, Ding JL. Iron-withholding strategy in innate immunity. Immunobiology 2006;211:295–314.
[25] Andrews SC, Arosio P, Bottke W, Briat JF, von Darl M, Harrison PM, et al. Structure, function, and evolution of ferritins. Journal of Inorganic Biochemistry 1992;47:161–74.
[26] von Darl M, Harrison PM, Bottke W. cDNA cloning and deduced amino acid sequence of two ferritins: soma ferritin and yolk ferritin, from the snail *Lymnaea stagnalis* L. European Journal of Biochemistry/FEBS 1994;222:353–66.
[27] Durand JP, Goudard F, Pieri J, Escoubas JM, Schreiber N, Cadoret JP. *Crassostrea gigas* ferritin: cDNA sequence analysis for two heavy chain type subunits and protein purification. Gene 2004;338:187–95.
[28] Zhang Y, Meng Q, Jiang T, Wang H, Xie L, Zhang R. A novel ferritin subunit involved in shell formation from the pearl oyster (*Pinctada fucata*). Comparative Biochemistry and Physiology Part B, Biochemistry & Molecular Biology 2003;135:43–54.
[29] De Zoysa M, Lee J. Two ferritin subunits from disk abalone (*Haliotis discus discus*): cloning, characterization and expression analysis. Fish & Shellfish Immunology 2007;23:624–35.
[30] Li J, Li L, Zhang S, Li J, Zhang G. Three ferritin subunits involved in immune defense from bay scallop *Argopecten irradians*. Fish & Shellfish Immunology 2012;32:368–72.
[31] Wang X, Liu B, Xiang J. Cloning, characterization and expression of ferritin subunit from clam *Meretrix meretrix* in different larval stages. Comparative Biochemistry and Physiology Part B, Biochemistry & Molecular Biology 2009;154:12–6.
[32] Li C, Li H, Su X, Li T. Identification and characterization of a clam ferritin from *Sinonovacula constricta*. Fish & Shellfish Immunology 2011;30:1147–51.
[33] Goulletquer P. A bibliography of the Manila clam *Tapes philippinarum*. IFREMER; 1997. RIDRV-9702/RA/La Tremblade, p. 122.
[34] Paillard C, Korsnes K, Le Chevalier P, Le Boulay C, Harkestad L, Eriksen AG, et al. *Vibrio tapetis*-like strain isolated from introduced Manila clams *Ruditapes philippinarum* showing symptoms of brown ring disease in Norway. Diseases of Aquatic Organisms 2008;81:153–61.
[35] Lee Y, Whang I, Umasuthan N, De Zoysa M, Oh C, Kang DH, et al. Characterization of a novel molluscan MyD88 family protein from Manila clam, *Ruditapes philippinarum*. Fish & Shellfish Immunology 2011;31:887–93.
[36] Thompson JD, Higgins DG, Gibson TJ. CLUSTAL W: improving the sensitivity of progressive multiple sequence alignment through sequence weighting, position-specific gap penalties and weight matrix choice. Nucleic Acids Research 1994;22:4673–80.
[37] Tamura K, Peterson D, Peterson N, Stecher G, Nei M, Kumar S. MEGA5: molecular evolutionary genetics analysis using maximum likelihood, evolutionary distance, and maximum parsimony methods. Molecular Biology and Evolution 2011;28:2731–9.
[38] Kaplan W, Littlejohn TG. Swiss-PDB viewer (Deep View). Briefings in Bioinformatics 2001;2:195–7.
[39] Maina CV, Riggs PD, Grandea 3rd AG, Slatko BE, Moran LS, Tagliamonte JA, et al. An *Escherichia coli* vector to express and purify foreign proteins by fusion to and separation from maltose-binding protein. Gene 1988;74:365–73.
[40] Bradford MM. A rapid and sensitive method for the quantitation of microgram quantities of protein utilizing the principle of protein–dye binding. Analytical Biochemistry 1976;72:248–54.
[41] Decker E, Welch B. Role of ferritin as a lipid oxidation catalyst in muscle foods. Journal of Agricultural and Food Chemistry 1990:4.
[42] Zheng WJ, Hu YH, Xiao ZZ, Sun L. Cloning and analysis of a ferritin subunit from turbot (*Scophthalmus maximus*). Fish & Shellfish Immunology 2010;28:829–36.
[43] Umasuthan N, Whang I, Lee Y, Lee S, Kim Y, Kim H, et al. Heparin cofactor II (RbHCII) from rock bream (*Oplegnathus fasciatus*): molecular characterization, cloning and expression analysis. Fish & Shellfish Immunology 2011;30:194–208.
[44] Waldo GS, Ling J, Sanders-Loehr J, Theil EC. Formation of an Fe(III)–tyrosinate complex during biomineralization of H-subunit ferritin. Science 1993;259:796–8.
[45] Orino K, Watanabe K. Molecular, physiological and clinical aspects of the iron storage protein ferritin. Veterinary Journal 2008;178:191–201.
[46] Ong DS, Wang L, Zhu Y, Ho B, Ding JL. The response of ferritin to LPS and acute phase of *Pseudomonas* infection. Journal of Endotoxin Research 2005;11:267–80.
[47] Beck G, Ellis TW, Habicht GS, Schluter SF, Marchalonis JJ. Evolution of the acute phase response: iron release by echinoderm (*Asterias forbesi*) coelomocytes, and cloning of an echinoderm ferritin molecule. Developmental and Comparative Immunology 2002;26:11–26.
[48] Xie M, Hermann A, Richter K, Engel E, Kerschbaum HH. Nitric oxide up-regulates ferritin mRNA level in snail neurons. The European Journal of Neuroscience 2001;13:1479–86.
[49] Hentze MW, Kuhn LC. Molecular control of vertebrate iron metabolism: mRNA-based regulatory circuits operated by iron, nitric oxide, and oxidative stress. Proceedings of the National Academy of Sciences of the United States of America 1996;93:8175–82.
[50] Zhang J, Li F, Wang Z, Zhang X, Zhou Q, Xiang J. Cloning, expression and identification of ferritin from Chinese shrimp, *Fenneropenaeus chinensis*. Journal of Biotechnology 2006;125:173–84.
[51] Surguladze N, Thompson KM, Beard JL, Connor JR, Fried MG. Interactions and reactions of ferritin with DNA. The Journal of Biological Chemistry 2004;279:14694–702.
[52] Jin C, Li C, Su X, Li T. Identification and characterization of a *Tegillarca granosa* ferritin regulated by iron ion exposure and thermal stress. Developmental and Comparative Immunology 2011;35:745–51.
[53] Ragg NL, Taylor HH. Oxygen uptake, diffusion limitation, and diffusing capacity of the bipectinate gills of the abalone, *Haliotis iris* (Mollusca: Prosobranchia). Comparative Biochemistry and Physiology Part A, Molecular & Integrative Physiology 2006;143:299–306.
[54] Andersen O, Dehli A, Standal H, Giskegjerde TA, Karstensen R, Rorvik KA. Two ferritin subunits of Atlantic salmon (*Salmo salar*): cloning of the liver cDNAs and antibody preparation. Molecular Marine Biology and Biotechnology 1995;4:164–70.
[55] Neves JV, Wilson JM, Rodrigues PN. Transferrin and ferritin response to bacterial infection: the role of the liver and brain in fish. Developmental and Comparative Immunology 2009;33:848–57.
[56] Rucker P, Torti FM, Torti SV. Role of H and L subunits in mouse ferritin. The Journal of Biological Chemistry 1996;271:33352–7.

[57] Zhang X, Wei W, Wu H, Xu H, Chang K, Zhang Y. Gene cloning and characterization of ferritin H and M subunits from large yellow croaker (*Pseudosciaena crocea*). Fish & Shellfish Immunology 2010;28: 735–42.
[58] Feng CY, Johnson SC, Hori TS, Rise M, Hall JR, Gamperl AK, et al. Identification and analysis of differentially expressed genes in immune tissues of Atlantic cod stimulated with formalin-killed, atypical *Aeromonas salmonicida*. Physiological Genomics 2009;37:149–63.
[59] Peatman E, Baoprasertkul P, Terhune J, Xu P, Nandi S, Kucuktas H, et al. Expression analysis of the acute phase response in channel catfish (*Ictalurus punctatus*) after infection with a Gram-negative bacterium. Developmental and Comparative Immunology 2007;31:1183–96.